Supplementary information for

The Role of Temperature and Adsorbate on Negative Gas Adsorption Transitions of the Mesoporous Metal-Organic Framework DUT-49

Simon Krause[1,2*], Jack D. Evans[1*], Volodymyr Bon[1], Irena Senkovska[1], François-Xavier Coudert[3], Daniel M. Többens[4], Dirk Wallacher[4], Nico Grimm[4], Stefan Kaskel[1*]

[1]Chair of Inorganic Chemistry, Technische Universität Dresden, Bergstrasse 66, 01062 Dresden, Germany

[2]Centre for Systems Chemistry, Stratingh Institute for Chemistry, University of Groningen, Nijenborgh 4, 9747 AG Groningen, The Netherlands

[3]Chimie ParisTech, PSL University, CNRS, Institut de Recherche de Chimie, Paris, 75005, Paris, France

[4]Helmholtz-Zentrum Berlin für Materialien und Energie, Hahn-Meitner-Platz 1, 14109, Berlin, Germany

*correspondence to: simon.krause@rug.nl, jack.evans@tu-dresden.de, stefan.kaskel@tu-dresden.de

Table of contents

1. Materials and methods 22
2. Low pressure adsorption experiments (<110 kPa) 23
3. High pressure adsorption experiments (1 kPa< *p* < 8 MPa) 24
4. Routine for sample recycling 25
5. Adsorption isotherms recorded in this study 26
6. Empirical analysis of NGA parameter 35
7. *In situ* PXRD experiments 38
8. Simulation methods 42
9. References 43

1. Materials and methods

The synthesis and characterization of this DUT-49 sample used in the presented experiments is in detail described in reference 1 where it is labelled as DUT-49(4). All samples used in the conducted study originate from the same batch of DUT-49 crystals with an average crystal size distribution of 4.26 µm. The following gases were used:

Supplementary Table 1. List of gases used for adsorption experiments.

Name	purity	Manufacturer
Helium	99.999	Linde
Argon	99.995%	Linde
Krypton	99%	Linde
Xenon	99.95%	Linde
Methane	99.995%	Linde
Ethene	99.9%	Linde
Ethane	99.9%	Linde
Propane	99.95%	Linde
n-Butane	99.95	Linde
iso-Butane	99.95	Praxair
1,3-Butandien	99%	Linde
Hydrogen	99.95%	Linde

Supplementary Table 2. List of solvents used for vapour adsorption experiments.

Name	purity	Manufacturer
n-Pentane	99% anhydr.	Sigma Aldrich
n-Hexane	99% anhydr.	Sigma Aldrich
n-Heptane	99% anhydr.	Sigma Aldrich

2. Low pressure adsorption experiments (<110 kPa)

Low pressure (p < 110 kPa) volumetric adsorption experiments were carried out on a BELSORP-max instrument by MICROTRACBEL CORP. and the measuring routine of BELSORP-max control software was used. In general, equilibration conditions for each point were 1% pressure change within at least 350 s. For adsorption experiments below the standard boiling point of the adsorptive 1% within 500 s was chosen. The dead volume was routinely determined using helium. Values for the adsorbed amount of gas in the framework are all given at STP and were recalculated to mmol g^{-1}. Prior to the measurement the samples were degassed at 373-423 K for at least 5 h in dynamic vacuum ($p < 10^{-4}$ kPa).

Vapor adsorption experiments were conducted at 298 K using the BELSORP-max routine for degassing and characterization of vapors. Equilibration criteria were increased to 0.5% pressure change within at least 550 s due to the low pressures and relatively slow equilibration in these experiments.

Several methods for reaching the desired adsorption temperatures were used: For analysis at 295 K or higher temperatures a JULABO thermostat was used. For analysis at 273 K ice was used as a coolant. To reach adsorption temperatures not achievable by these techniques in the range of 10 K – 300 K a closed cycle helium cryostat was used. The cryostat DE-202AG was operated by a temperature controller LS-336 (LAKE SHORE) and the heat produced by the cryostat is removed from the system by a water-cooled helium compressor ARS-2HW. The sample was placed in a custom made cell consisting of a 3 cm long rod-shaped copper cell of 1 cm diameter, sealed from the exterior with a copper dome and insulated by dynamic vacuum ($p < 10^{-4}$ kPa), and connected to the BELSORP-max adsorption instrument with a 1.5 mm copper capillary. The samples were degassed prior to the measurement at room temperature for at least 1 h in dynamic vacuum ($p < 10^{-7}$ kPa).

3. High pressure adsorption experiments (1 kPa< *p* < 8 MPa)

High pressure (1 kPa< *p* < 8 MPa) volumetric adsorption experiments were carried out on a BELSORP-HP instrument by MICROTRACBEL CORP. and the measuring routine of BELSORP-HP control software was used. In general equilibration conditions for each point were 1% pressure change within at least 350 s (exceptions are mentioned specifically). The dead volume was routinely determined using helium at 298 K and at the desired adsorption temperature. The adsorption temperatures in the range of 10 K – 300 K were achieved by using the same closed cycle helium cryostat described in detail above. The sample was placed in a custom-made cell consisting of 3 cm long stainless-steel SWAGELOK cell of 0.5 cm inner diameter and connected to the BELSORP-HP adsorption instrument with a 0.5 mm stainless steel capillary. The cell was insulated by dynamic vacuum ($p < 10^{-4}$ kPa), and the samples were degassed prior to the measurement at room temperature for at least 1 h in dynamic vacuum ($p < 10^{-5}$ kPa). Adsorbed amounts are given as excess amount adsorbed in mmol g^{-1}.

4. Routine for sample recycling

In our previous studies on NGA the transition upon desorption was found to be irreversible[2]. Consequently, for each adsorption measurement a new sample of DUT-49 had to be used to record individual isotherms. To overcome this extensive usage of sample amount a routine was developed to cycle DUT-49 even when NGA is present. This procedure was previously described in two references[2, 3] and was primarily applied in the characterization of methane and ethane for which experiments were first conducted at elevated temperatures and then stepwise decreased until structural transitions were observed and then after desorption the regeneration protocol applied.

In general, some adsorbed molecules can be removed from the pores of DUT-49 if the guest molecules are in a supercritical state. This fact is used in the initial supercritical activation of DUT-49 using carbon dioxide. When analyzing the adsorption behavior upon adsorption of methane it becomes obvious that the isotherms become reversible at temperatures beyond the critical point (for methane around 150 K). Thus, methane can be removed from the pores of DUT-49*op* by increasing the temperature beyond this point while maintaining saturation pressure in the measuring cell. This method of regeneration has some experimental limitations: The increase in temperature while maintaining saturation pressure of the adsorptives can lead to high pressures. Thus, this method of regeneration could only be performed in high pressure equipment. For experiments conducted at pressures below 100 kPa in the BELSORP-max instrument, each experiment was performed on a fresh sample. In addition, this recycling technique was found to be not applicable to adsorption of krypton, propane, *n*-butane (due to limitations of upper temperature limit of the instrument) and ethene.

5. Adsorption isotherms recorded in this study

In the following figures adsorption isotherms of different gases/vapors and recorded at different temperatures are depicted. In each isotherm filled symbols correspond to the adsorption, empty symbols to the desorption carried out subsequently.

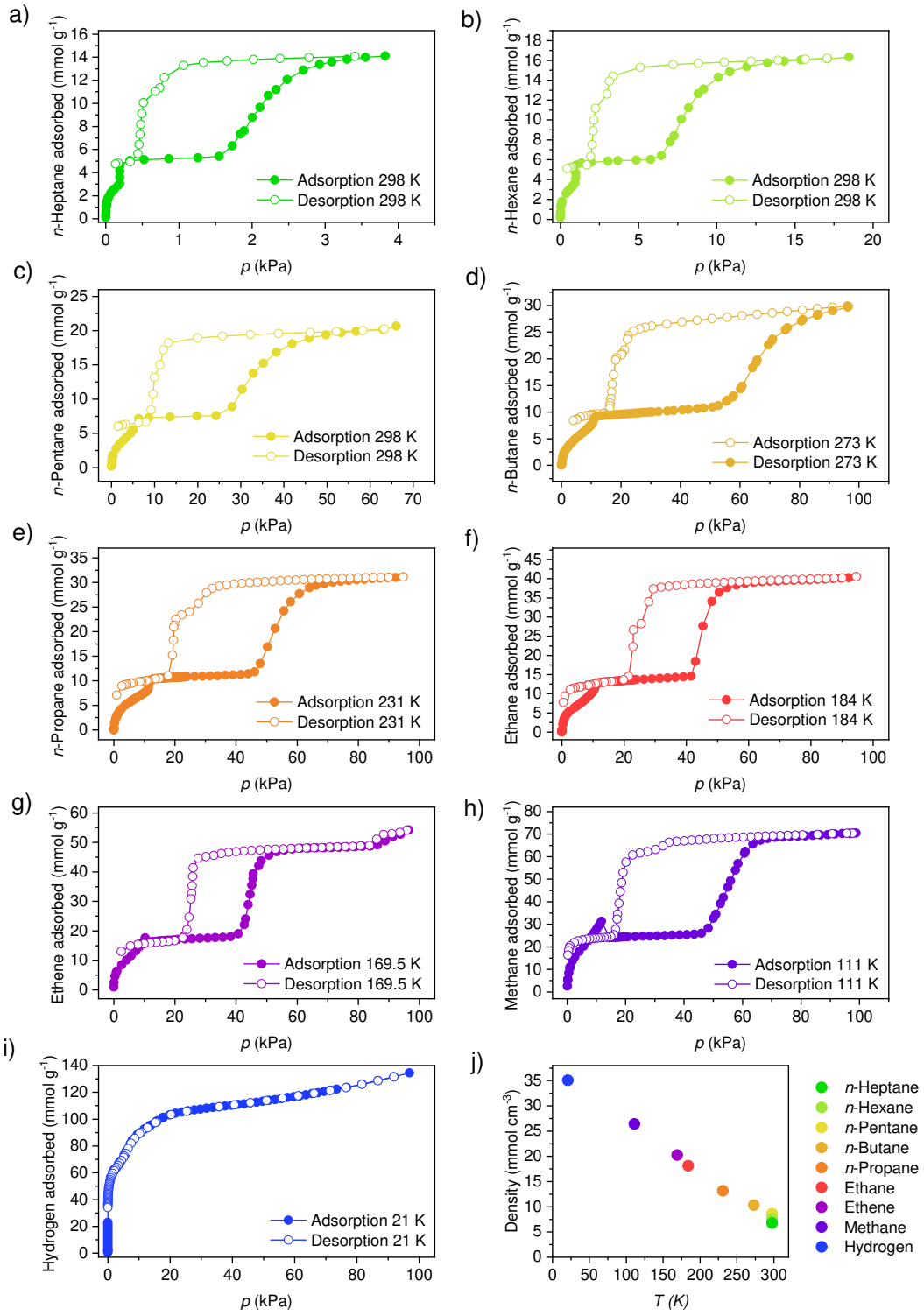

Supplementary Figure 1. Adsorption (closed circles) and desorption (open circles) isotherms of a) *n*-heptane, b) *n*-hexane, c) *n*-pentane, d) *n*-butane, e) *n*-propane, f) ethane, g) ethene, h) methane, and i)

hydrogen at their respective boiling points with the exception of vaporized *n*-pentane-*n*-heptane in DUT-49j) Molar density of fluid adsorptive at adsorption temperature and saturation pressure, methane and ethene are the only two gases to show NGA.

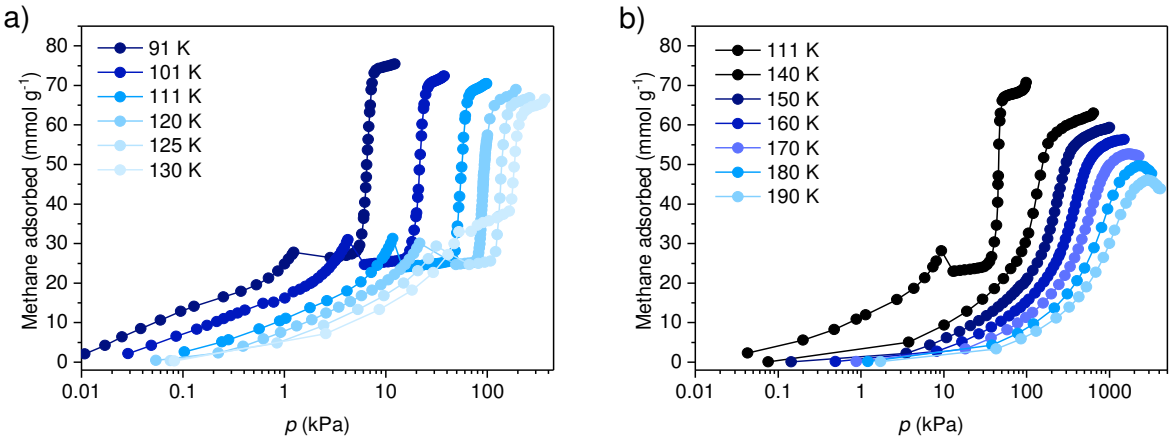

Supplementary Figure 2. Adsorption iisotherms of methane in DUT-49 at a) 91-130 K and b) 140-190 K including 111 K for comparison.

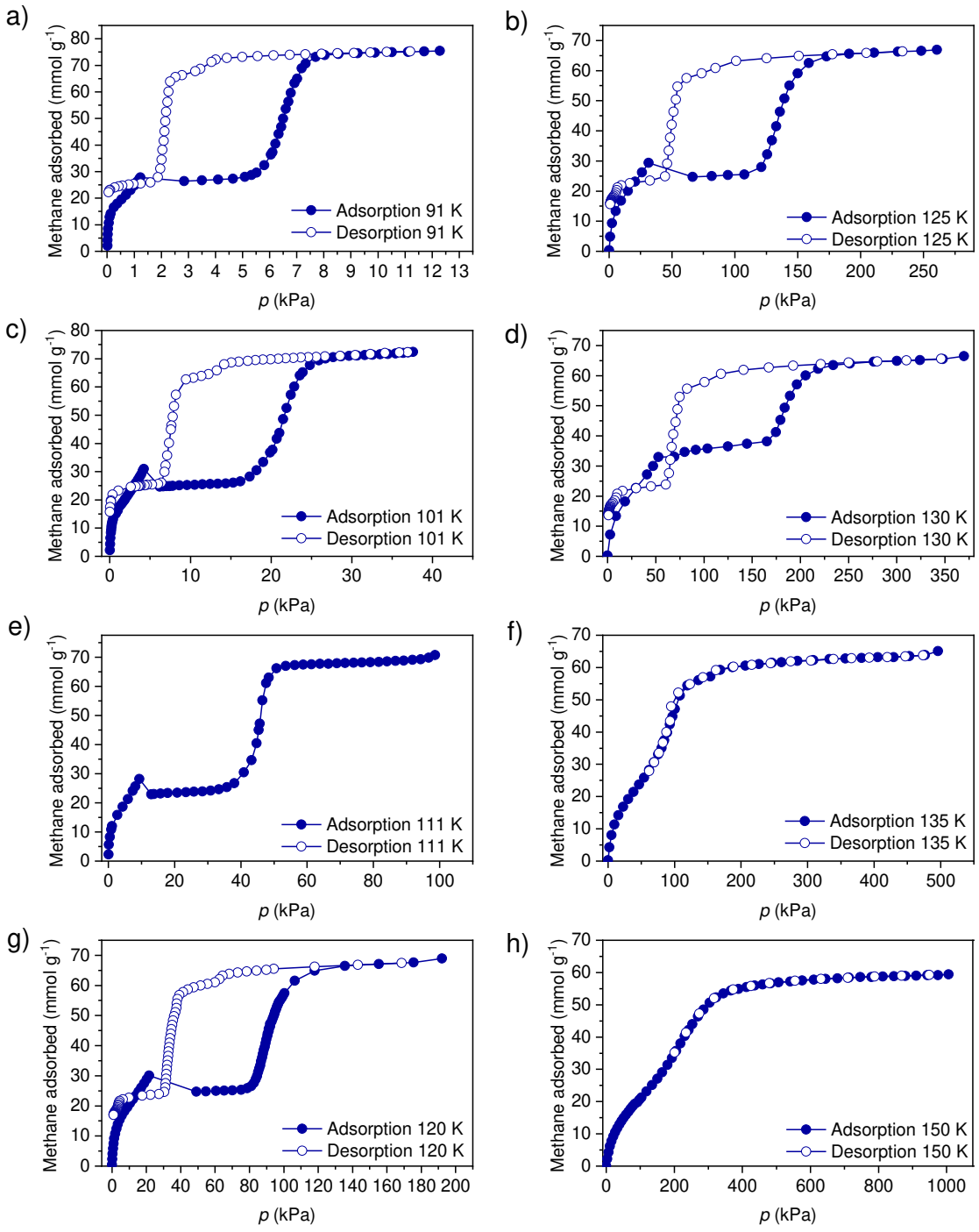

Supplementary Figure 3. Methane adsorption/desorption isotherms on DUT-49 at a) 91 K, c) 101 K, e) 111 K, g) 120 K, b) 125 K, d) 130 K, f) 135 K, and h) 150 K. Adsorption in closed symbols, desorption in open symbols.

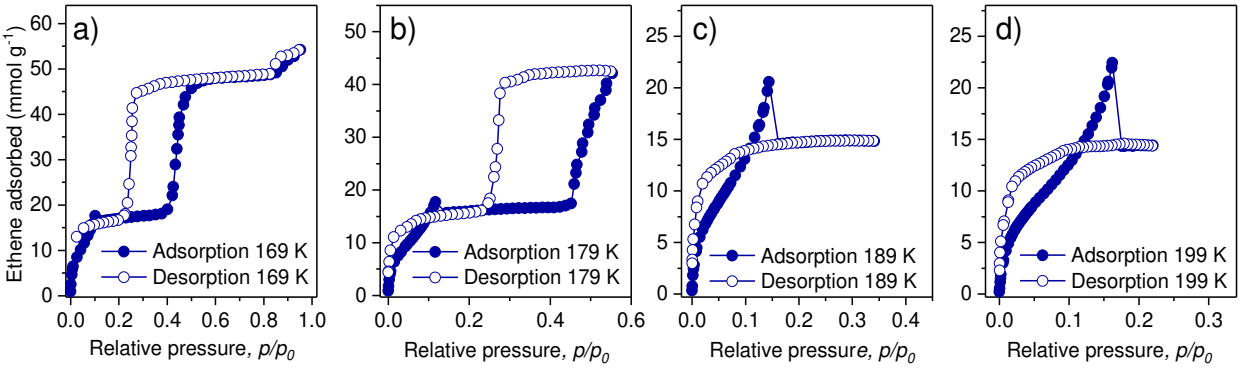

Supplementary Figure 4. Adsorption (closed symbols) and desorption (open symbols) isotherms of ethene at a) 169 K, b) 179 K, c) 189 K, and d) 199 K in DUT-49.

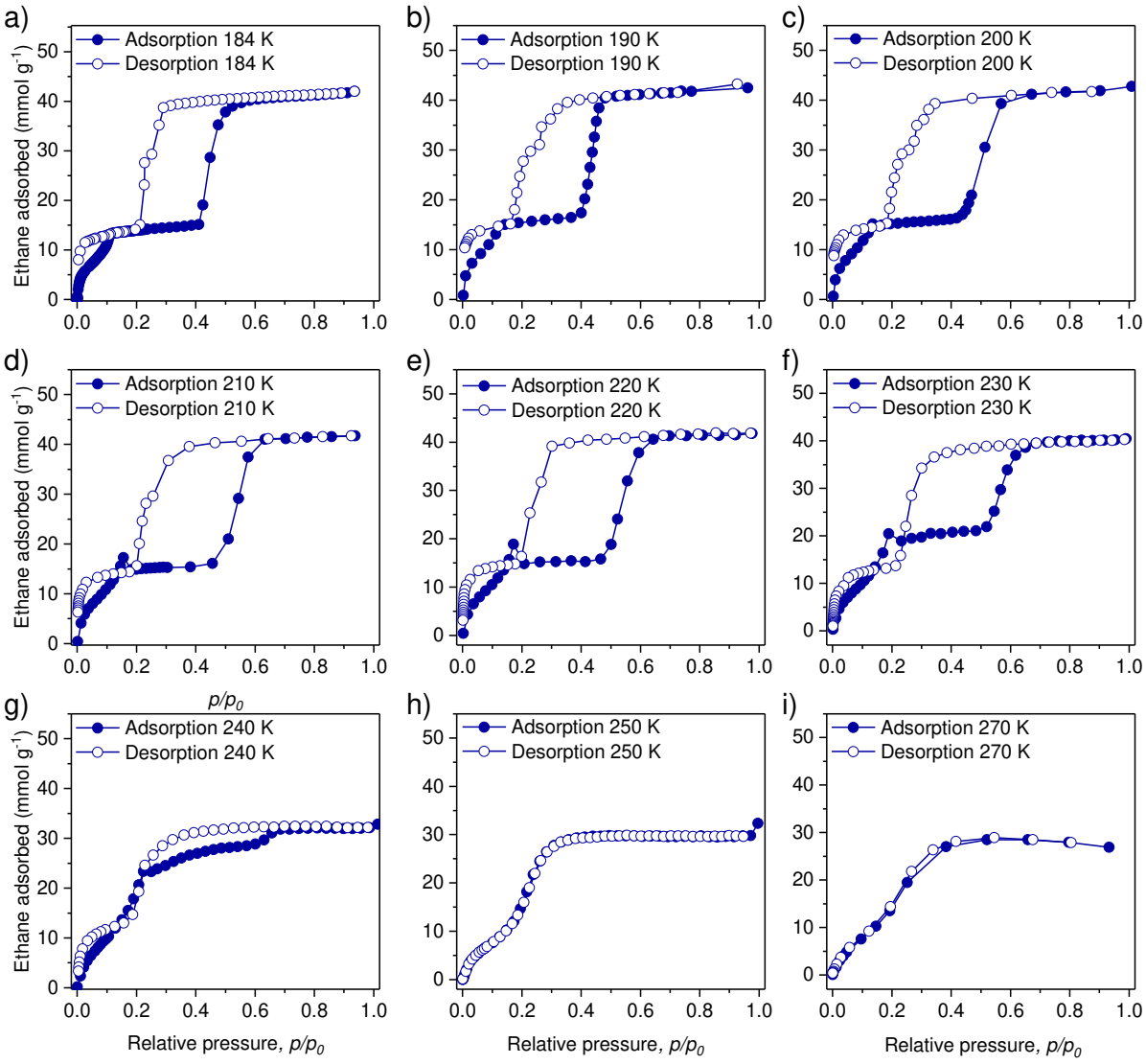

Supplementary Figure 5. Adsorption (closed symbols) and desorption (open symbols) isotherms of ethane at a) 184 K, b) 190 K, c) 200 K, d) 210 K, e) 220 K, f) 230 K, g) 240 K, h) 250 K, and i) 270 K in DUT-49.

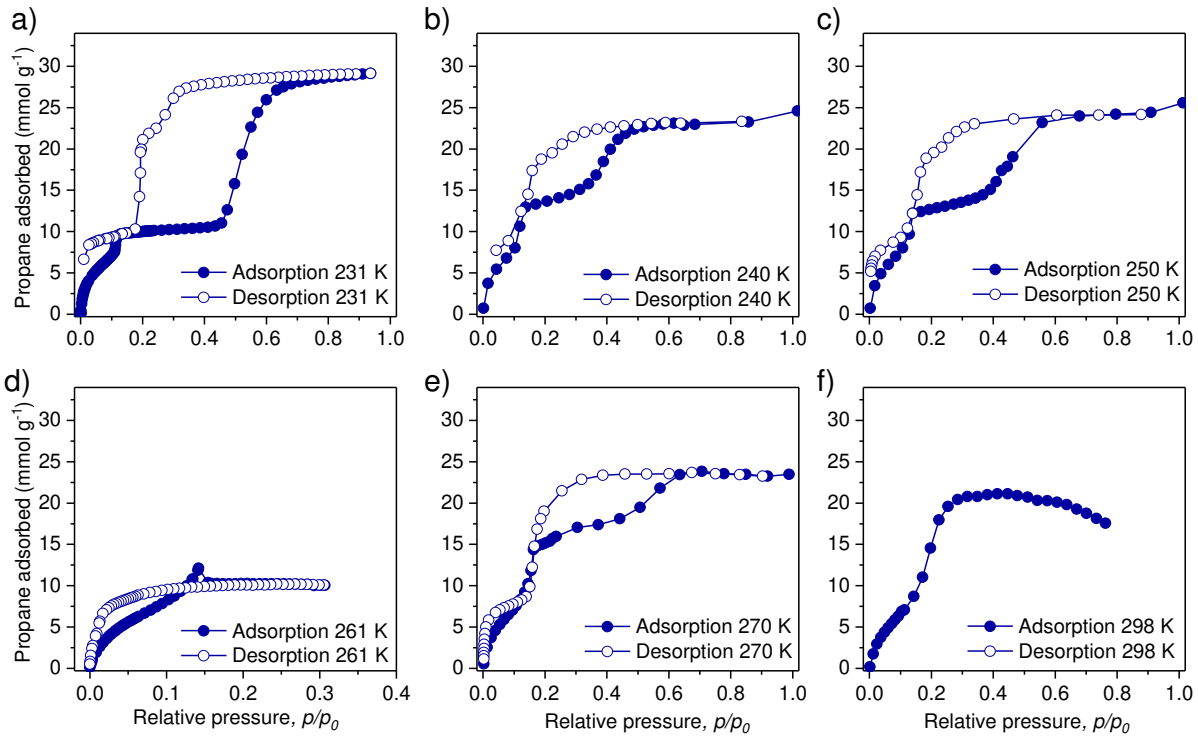

Supplementary Figure 6. Adsorption (closed symbols) and desorption (open symbols) isotherms of propane at a) 231 K, b) 240 K, c) 250 K, d) 261 K, e) 270 K, and f) 298 K in DUT-49.

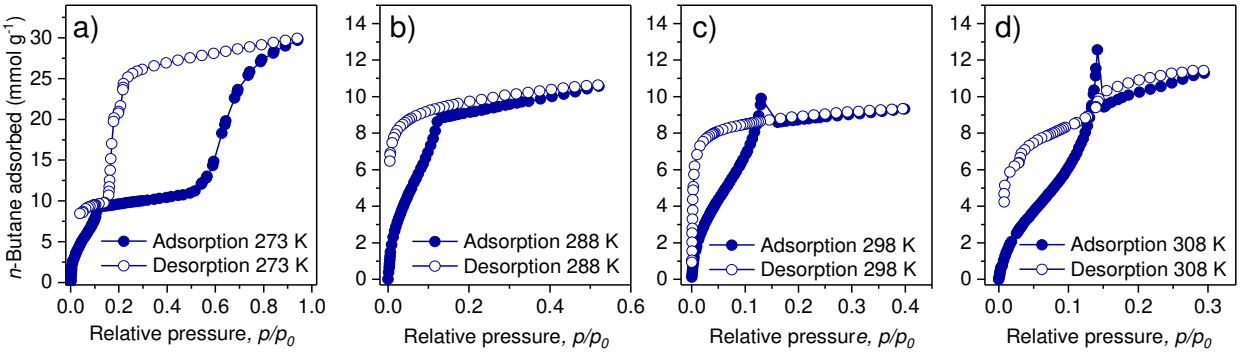

Supplementary Figure 7. Adsorption (closed symbols) and desorption (open symbols) isotherms of *n*-butane at a) 273 K, b) 288 K, c) 298 K, and d) 308 K in DUT-49.

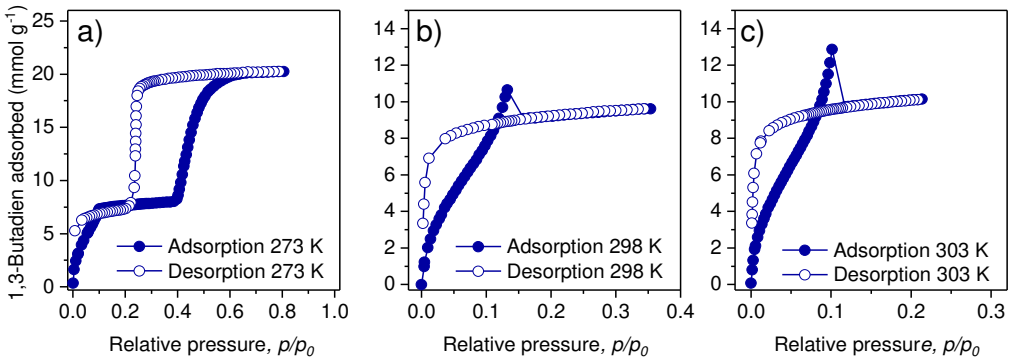

Supplementary Figure 8. Adsorption (closed symbols) and desorption (open symbols) isotherms of 1,3-butadiene at a) 273 K, b) 298 K, and c) 303 K in DUT-49.

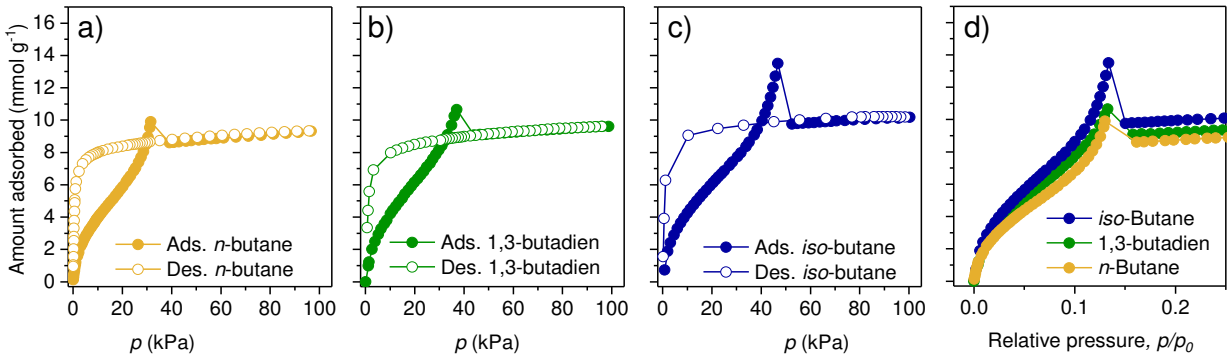

Supplementary Figure 9. Adsorption (closed symbols) and desorption (open symbols) isotherms of a) *n*-butane (yellow), b) 1,3-butadien (green), c) *iso*-butane (blue), and comparison of adsorption branches at 298 K.

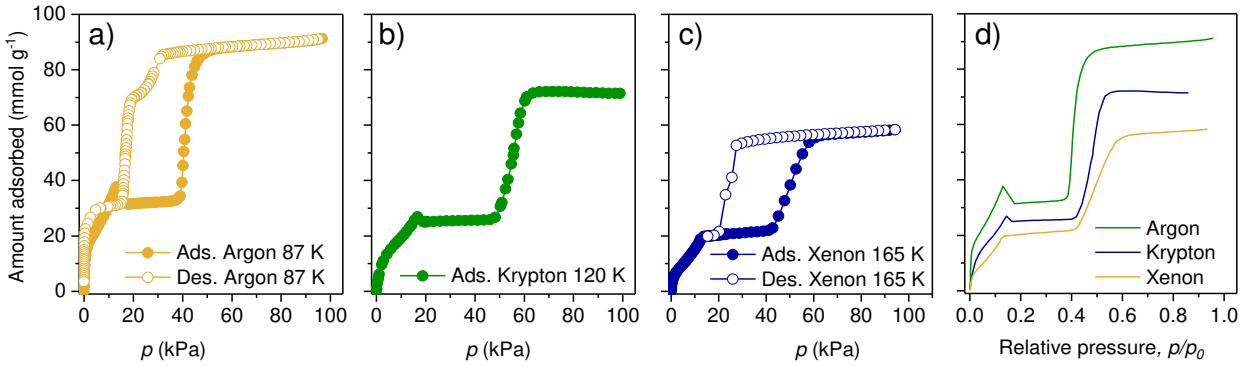

Supplementary Figure 10. Adsorption (closed symbols) and desorption (open symbols) isotherms of a) argon at 87 K, b) krypton at 120 K, c) xenon at 165 K, and d) direct comparison of the adsorption branches.

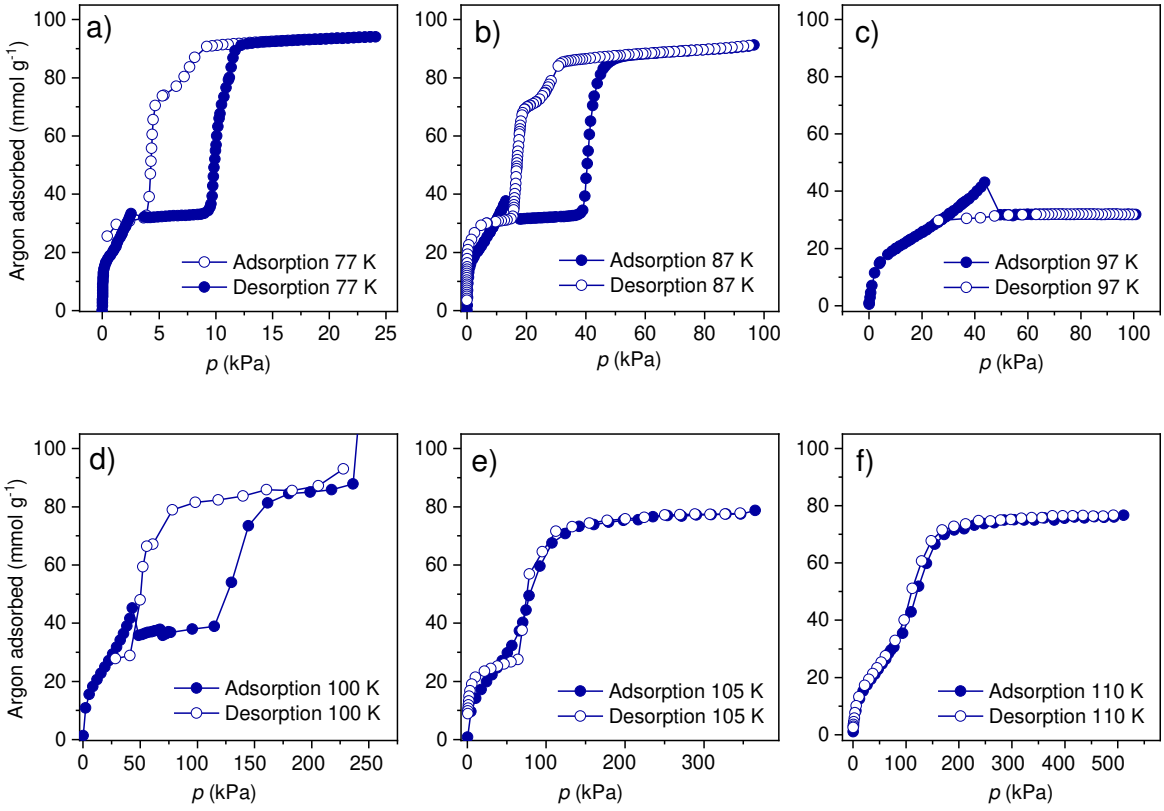

Supplementary Figure 11. Adsorption (closed symbols) and desorption (open symbols) isotherms of argon at a) 77 K, b) 87 K, c) 97 K, and d) 100 K, e) 105 K, and f) 110 K.

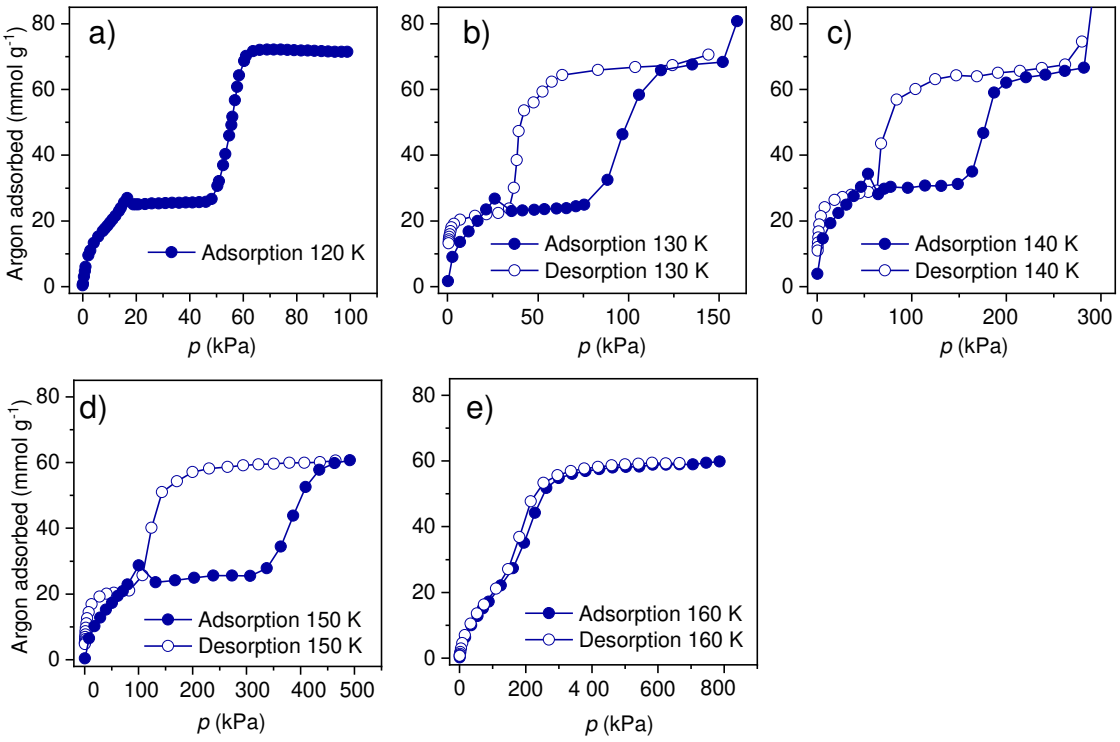

Supplementary Figure 12. Adsorption (filled symbols) and desorption (empty symbols) isotherms of krypton at a) 120, b) 130 K, c) 140 K, d) 150 K, and e) 160 K.

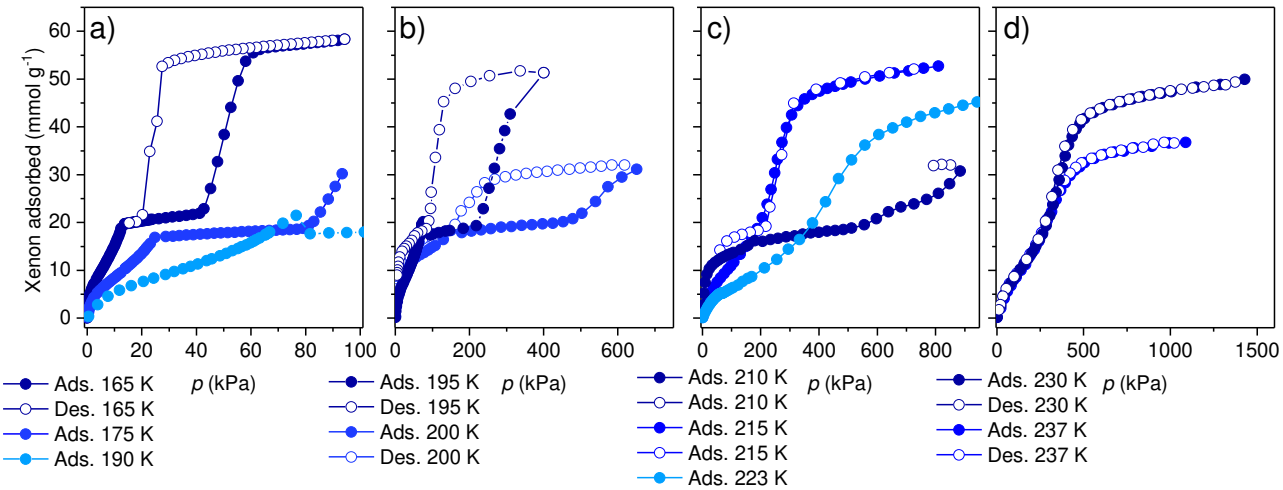

Supplementary Figure 13. Adsorption (filled symbols) and desorption (empty symbols) isotherms of xenon at a) 165 K,175 K, and 190 K, b) 195 and 200 K, c) 210 K, 215 K, and 237 K, and d) 230 K and 237 K.

6. Empirical analysis of NGA parameter

NGA parameters were derived from the previously shown isotherms. In the table below numerical values relevant for the discussion of the manuscript are provided in Supplementary Table 3. It is important to note that adsorption experiments may suffer from errors primarily caused by variations in the sample amount and inaccurate weighing caused by the preparation under inert atmosphere. A second inaccuracy originated from the resolution of the isotherms which, in the case of high-pressure isotherms, strongly relies on the sample amount used in the experiment. This inaccuracy is expected to result in an underestimation of ΔnNGA. Temperature accuracy in the conducted experiments was determined by internal calibration via condensation of the fluid at saturation pressure. The instrument itself provides a high temperature stability and accuracy of 0.01 K.

Supplementary Table 3. contains the adsorption temperature, *T*, the adsorbed amount in the *op* phase before NGA, n_{op}(NGA), the adsorbed amount in the *cp* phase after NGA, *n*cp(NGA), the amount of gas expelled upon NGA expressed as ΔnNGA, as well as the pressure at which NGA occurs, *p*NGA, recorded at n_{op}(NGA).

Supplementary Table 3. Numerical values to describe NGA properties derived from the recorded isotherms.

Gas	*T* (K)	n_{op}(NGA) (mmol g^{-1})	n_{cp}(NGA) (mmol g^{-1})	Δn_{NGA} (mmol g^{-1})	p_{NGA} (kPa)
Methane	91	27.82	26.45	1.37	1.23
	101	30.96	24.67	6.28	4.23
	111	28.15	22.93	6.12	9.39
	120	30.09	24.7	5.39	21.62
	125	29.36	24.71	4.66	31.53
	130	33.061	32.99	0.07	52.87
Ethene	169	17.6	16.37	1.23	10.25
	179	17.69	15.64	2.05	20.29
	189	20.57	14.54	6.02	40.67
	199	22.41	14.33	8.08	71.01
Ethane	200	15.14	14.92	0.22	29.44
	210	17.27	14.85	2.42	52.03
	220	18.86	14.83	4.02	84.75
	230	20.42	18.93	1.49	132.9
	240	23.35	23.27	0.08	216.3
Propane	261	12.12	10.35	1.76	45.61
n-Butane	288	9.21	8.86	0.35	22.38
	298	9.9	8.59	1.31	31.51
	308	12.55	9.43	3.12	46.24
1,3-Butadiene	298	10.64	9.07	1.57	37.05
	303	12.85	9.71	3.13	46.56
2-Methylpropane	298	46.24	9.75	3.76	46.73
Argon	77	33.35	32.19	1.15	3.714
	87	37.69	31.43	6.26	13.12
	97	43.12	31.77	11.3	43.68
Krypton	100	45.24	35.75	9.49	43.26
	120	26.93	25.04	1.88	16.63
	130	26.73	23.01	3.72	26.08
	140	34.36	28.13	6.23	53.84
	150	28.67	23.58	5.09	100.53
Xenon	195	21.5	17.64	3.85	76.55
	200	20.13	17.37	2.75	75.82
	210	18.29	17.89	0.39	112.21
	215	16.18	16.06	0.12	134.95

Critical temperatures, T_c, and standard boiling points, T_b, of the gases used in the experiments were obtained from the NIST Chemistry webBook SRD 69 (https://webbook.nist.gov/chemistry/fluid/) and are listed in the following table.

Supplementary Table 4. Critical temperatures and standard boiling points of gases used in the experiments.

Gas	Critical temperature, T_c (K)	Standard boiling point, T_b (K)
Methane	190.6	111.7
Ethene	282.3	169.4
Ethane	305.3	184.5
Propane	369.8	231
n-Butane	425.1	272.6
1,3-Butadiene	425.1	268.8
2-Methylpropane	407.8	261.4
Argon	150.7	87.3
Krypton	209.5	119.7
Xenon	289.7	165

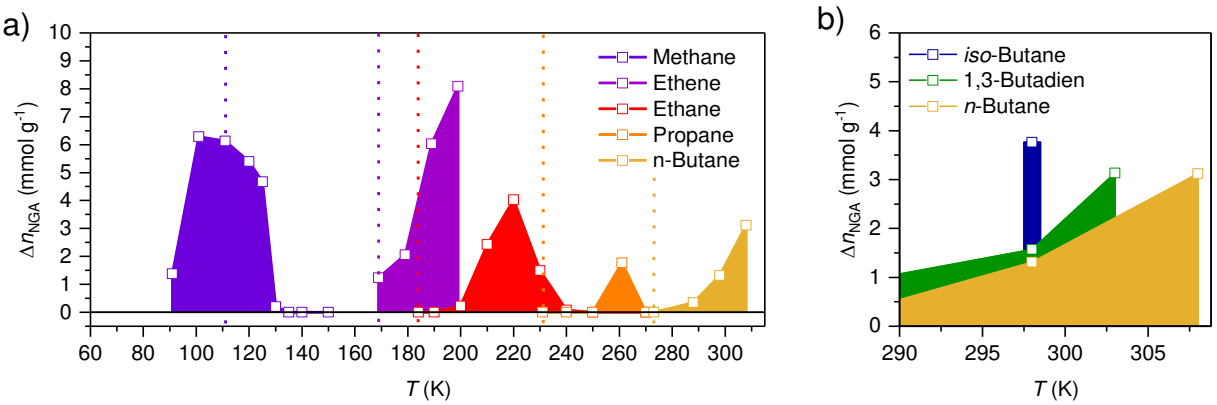

Supplementary Figure 14. Temperature-depending presence and magnitude of Δn_{NGA} in DUT-49 for different hydrocarbons. a) Linear saturated hydrocarbons with respective boiling points indicated as dashed vertical lines, b) butane derivatives at near ambient temperatures.

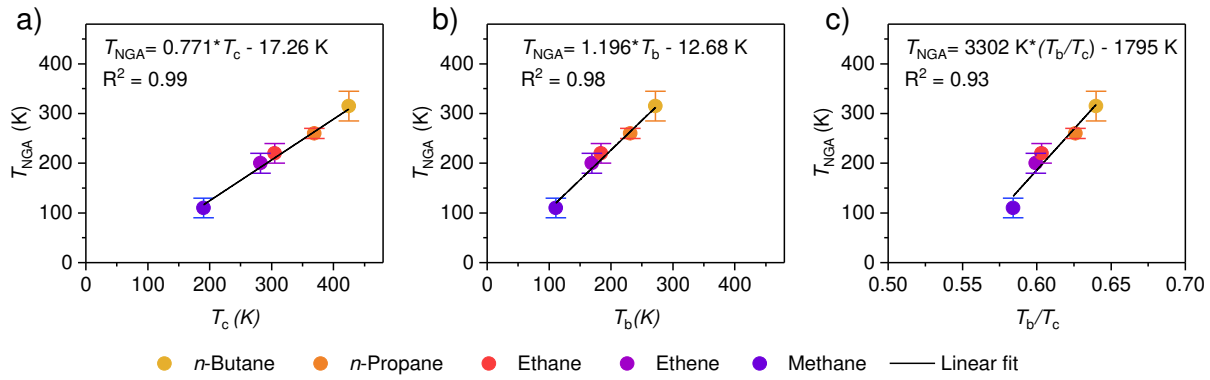

Supplementary Figure 15. T_{NGA} plotted over a) critical temperature, b) standard boiling point, and c) reduced temperature. Linear fits for each plot and error bars are provided.

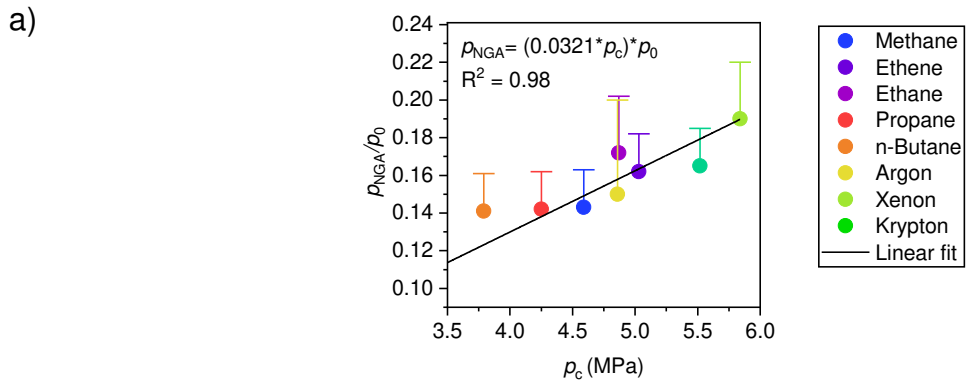

Supplementary Figure 16. Relationship of critical pressure p_c and relative pressure of NGA p_{NGA}/p_0, for all presented gases including parameters for linear fit.

7. *In situ* PXRD experiments

PXRD experiments in parallel to adsorption were performed at BESSY II light source, KMC-2 beamline of Helmholtz-Zentrum Berlin für Materialien und Energie[4] using the recently established experimental setup.[5] The diffraction experiments were performed in transmission geometry using a sample holder with a thickness of 2 mm. Monochromatic radiation with energy of 8048 eV (λ = 1.5406 Å) was used for all experiments. The diffraction images were measured using 2θ scan mode and a Vantec 2000 area detector system (BRUKER) in the range of 2 – 50° 2θ. A synchrotron beam with dimensions of 0.5 x 0.5 mm was used for the experiments. Corundum powder with a crystallite size of 5 µm was used as an external standard. The image frames were integrated using Datasqueeze 2.2.9 software[6] and processed using Fityk 0.9.8 program[7].

To control the gas loading the BELSORP-max setup was used. The adsorption chamber was sealed with an X-ray transparent beryllium dome and connected to the BELSORP-max via a 1.5 mm copper capillary. The adsorption cell was isolated by a second beryllium dome and insulating dynamic vacuum ($p < 10^{-5}$ kPa). Different gas loadings were dosed to the cell and equilibrated by using either the automated BELSORP software while automatically recording a full isotherm or by manually dosing. The gas pressure was equilibrated for at least 400 s before a PXRD pattern was recorded in both cases. The adsorption temperature was controlled by a closed cycle helium cryostat. The cryostat DE-202AG was operated by a temperature controller LS-336 (LAKE SHORE) and the heat produced by the cryostat is removed from the system by a water-cooled helium compressor ARS-2HW.

Temperature dependent PXRD experiments were performed in a closed chamber under dynamic vacuum of 10^{-4} mbar in the temperature range of 100 – 725 K with steps of 25 K on a PANALYTICAL X'PERT PRO with λ = 0.15405 nm in Bragg-Brentano-geometry. The temperature was raised with 5 K min^{-1} starting at 100 K. For each temperature three PXRD patterns were collected under isothermal conditions in the 2Θ range from 2.5 up to 22 °, with a step size of 0.028 ° and 40 s per step.

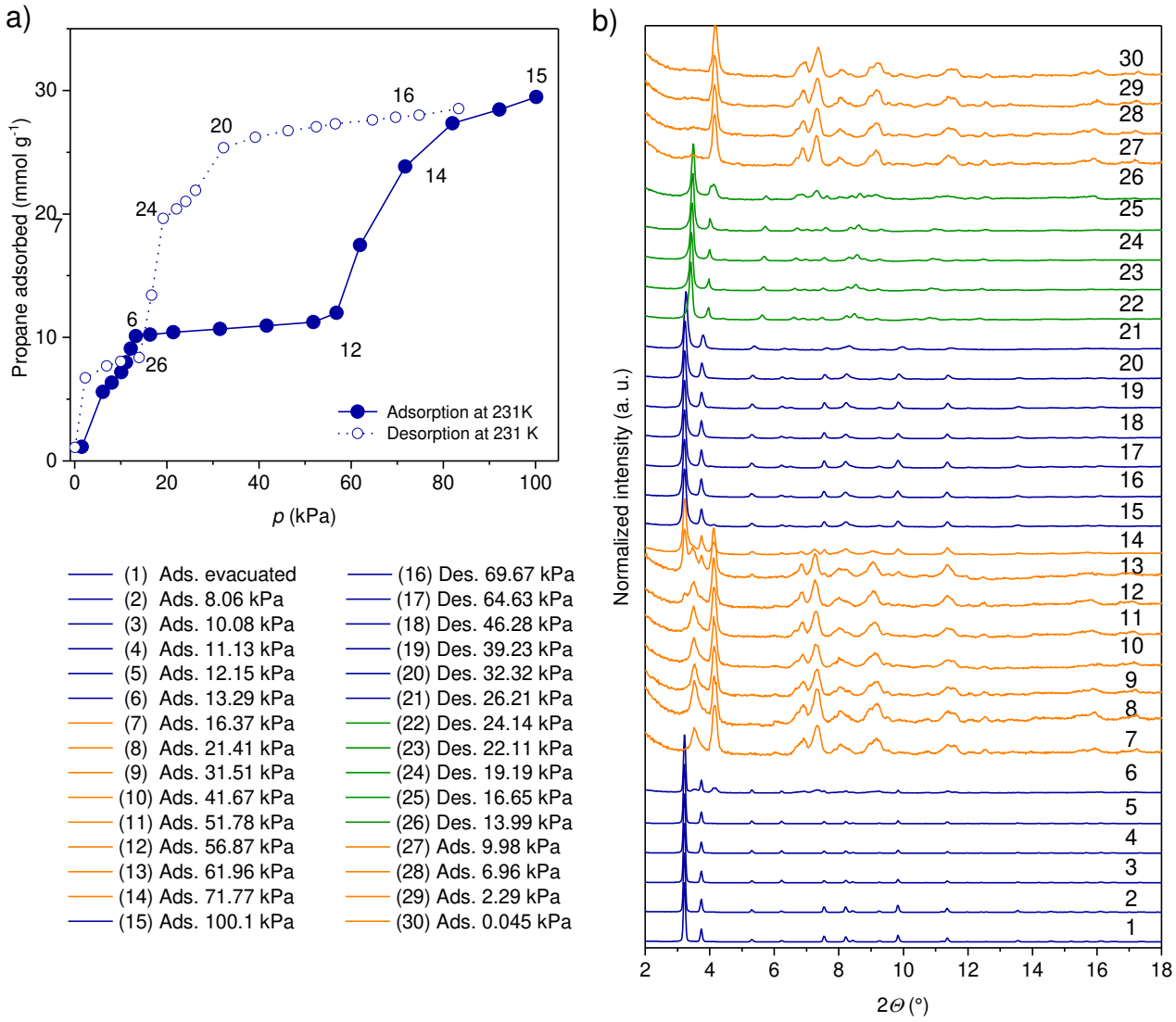

Supplementary Figure 17. *In situ* PXRD in parallel to propane physisorption at 231 K of DUT-49: Adsorption-desorption isotherm (a), selected points are labeled by numbers. Filled symbols correspond to adsorption, empty symbols to desorption. b) PXRD patterns, color code: DUT-49*cp* (orange) DUT-49*ip* (green), and DUT-49*op* (blue).

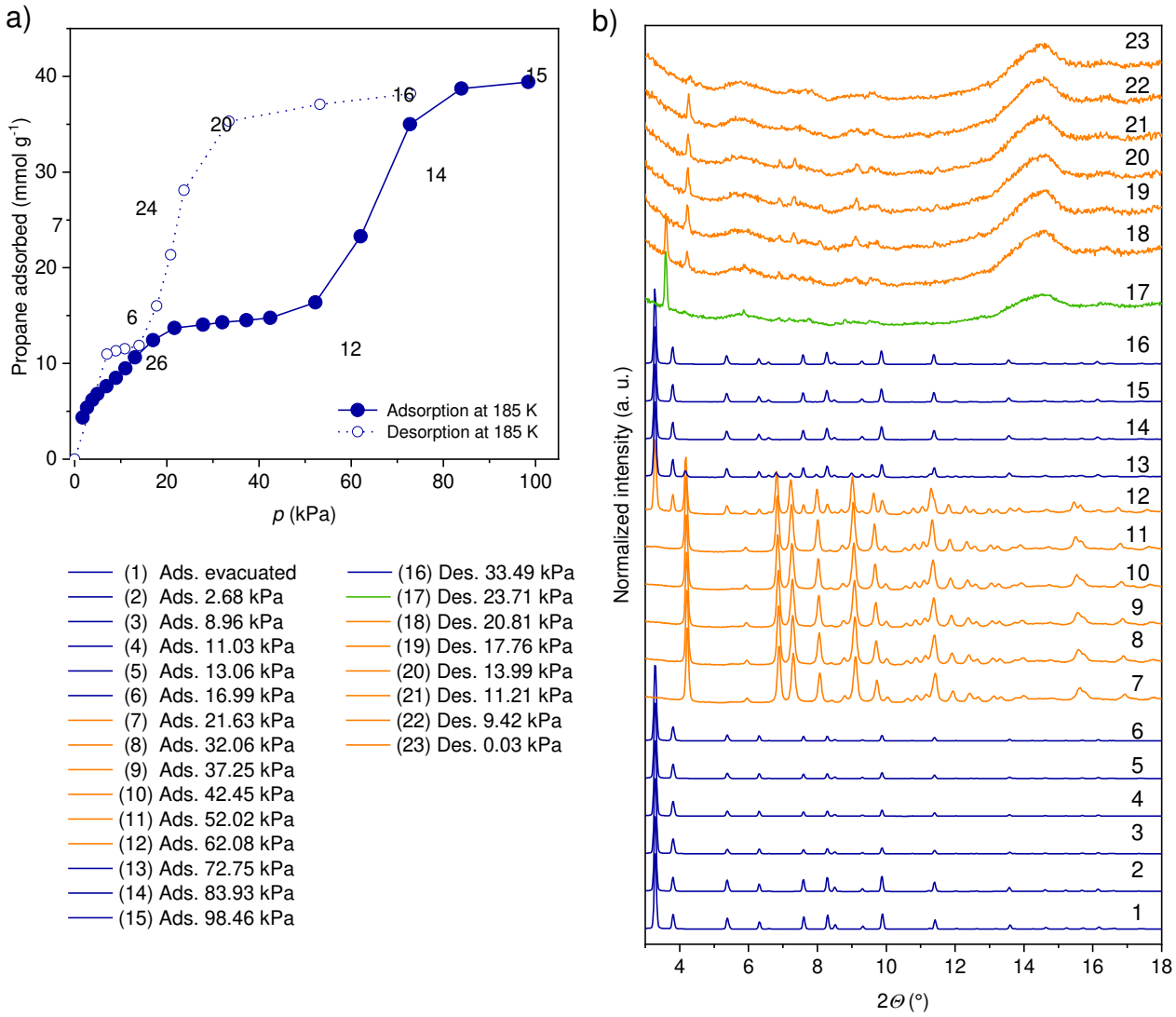

Supplementary Figure 18. *In situ* PXRD in parallel to ethane physisorption at 185 K of DUT-49: Adsorption-desorption isotherm (a), selected points are labeled by numbers. Filled symbols correspond to adsorption, empty symbols to desorption. b) PXRD patterns, color code: DUT-49*cp* (orange) DUT-49*ip* (green), and DUT-49*op* (blue).

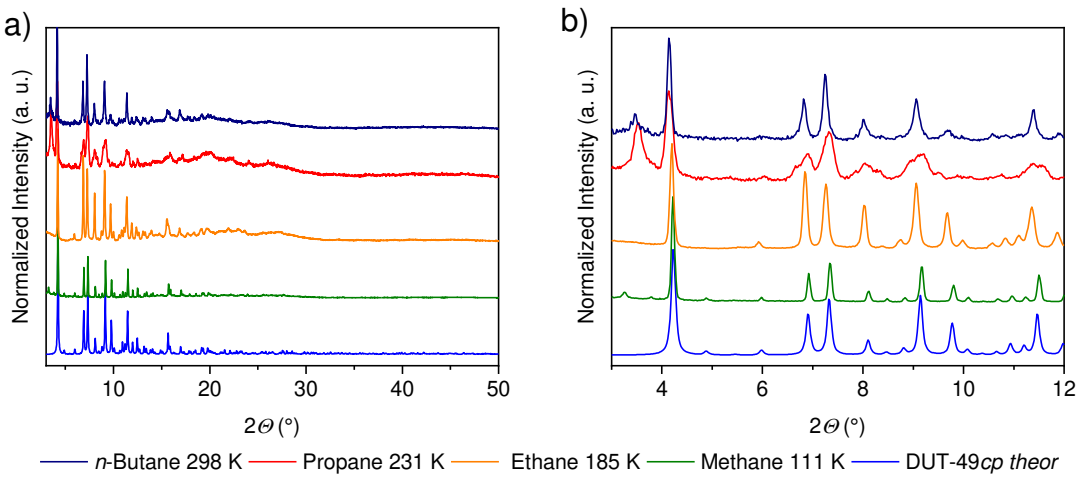

Supplementary Figure 19. PXRD patterns simulated for DUT-49cp (blue), an *in situ* pattern of methane adsorbed at DUT-49 at 111 K and 14 kPa (green), ethane adsorbed at 185 K and 21.6 kPa (orange), propane adsorbed at 231 K and 13 kPa (red), and *n*-butane adsorbed at 298 K and 41 kPa (dark blue). b) Enlargement of low angle region.

8. Simulation methods

Grand canonical Monte Carlo (GCMC) simulations used the RASPA2.0 code[8] and simulated the adsorption for previously reported *op* and *cp* structures of DUT-49. Each isotherm was simulated with an equilibration of 5×10^5 cycles and the subsequent 1×10^6 cycles were sampled, for each pressure point. A total of 50 pressures were investigated for each temperature and were uniformly distributed in log space between 1×10^{-2} Pa and 5×10^6 Pa. For each simulation, the van der Waals interactions for the framework used the UFF force field[9] and methane the united-atom TraPPe force field.[10] Parameters for framework-gas interactions were obtained by Lorentz–Berthelot mixing rules. No charges were considered for the framework atoms.

We computed the osmotic ensemble from interpolation of the simulated isotherms. In particular, we consider the difference in osmotic potential between the *op* and *cp* forms (fi), without considering the difference in energy of the host. This provides the energy gained by the phase transformation *op*→*cp*.

Adsorption stress was simulated using the MOF-FF[11] and united-atom TraPPe[10] force fields to describe DUT-49 and methane, respectively. Trajectories were computed in the *NVT* ensemble, using lammps[12], employing the Nose-Hoover thermostat with a dampening parameter of 100 fs and a timestep of 1 fs. Starting configurations were obtained from snapshots of GCMC simulations, described previously, and 10 unique configurations were sampled for each loading. The trajectories were simulated for a total of 1000 ps and the last 500 ps were used for sampling the total stress of the system. To provide greater precision in the area of NGA, l6 loadings between 400 and 700 methane molecules were simulated, using the same methodology, however, 50 unique configurations were sampled.

Please note, raw data and representative input files for molecular simulations described here are available online in our data repository at https://github.com/ jackevansadl/supp-data.

9. References

1. S. Krause, V. Bon, I. Senkovska, D. M. Többens, D. Wallacher, R. S. Pillai, G. Maurin and S. Kaskel, *Nat. Commun.*, 2018, **9**, 1573.
2. S. Krause, V. Bon, I. Senkovska, U. Stoeck, D. Wallacher, D. M. Többens, S. Zander, R. S. Pillai, G. Maurin, F. o.-X. Coudert and S. Kaskel, *Nature*, 2016, **532**, 348-352.
3. S. Krause, J. D. Evans, V. Bon, I. Senkovska, P. Iacomi, F. Kolbe, S. Ehrling, E. Troschke, J. Getzschmann, D. M. Többens, A. Franz, D. Wallacher, P. G. Yot, G. Maurin, E. Brunner, P. L. Llewellyn, F.-X. Coudert and S. Kaskel, *Nat. Commun.*, 2019, **10**, 3632.
4. Helmholtz-Zentrum Berlin für Materialien und Energie, *JLSRF*, 2016, **2**, A49.
5. R. Grunker, V. Bon, P. Muller, U. Stoeck, S. Krause, U. Mueller, I. Senkovska and S. Kaskel, *Chem. Commun.*, 2014, **50**, 3450-3452.
6. P. A. Heiney, *Journal*, 2012.
7. M. Wojdyr, *J. Appl. Crystallogr.*, 2010, **43**, 1126-1128.
8. D. Dubbeldam, S. Calero, D. E. Ellis and R. Q. Snurr, *Molecular Simulation*, 2016, **42**, 81-101.
9. A. K. Rappe, C. J. Casewit, K. S. Colwell, W. A. Goddard and W. M. Skiff, *J. Am. Chem. Soc.*, 1992, **114**, 10024-10035.
10. M. G. Martin and J. I. Siepmann, *J. Phys. Chem. B*, 1998, **102**, 2569-2577.
11. S. Bureekaew, S. Amirjalayer, M. Tafipolsky, C. Spickermann, T. K. Roy and R. Schmid, *Phys. Status Solidi B*, 2013, **250**, 1128-1141.
12. S. Plimpton, *Journal of Computational Physics*, 1995, **117**, 1-19.